

RESEARCH ARTICLE

## The Impact of Nano-Sized Gold Particles on the Target Dose Enhancement Based on Photon Beams Using by Monte Carlo Method

Hossein Khosravi<sup>1\*</sup>; Armita Mahdavi Gorabi<sup>2</sup>; Faezeh Rahmani<sup>3</sup>; Ahmad Ebadi<sup>1</sup>

<sup>1</sup>Health Institute, Chamran Hospital, Tehran, Iran

<sup>2</sup>Department of Basic and Clinical Research, Tehran Heart Center, Tehran University of Medical Sciences, Tehran, Iran

<sup>3</sup>Department of Physics, K. N. Toosi University of Technology, Tehran, Iran

### ARTICLE INFO

#### Article History:

Received 15 May 2016;

Accepted 28 July 2016;

Published 09 August 2016

#### Keywords:

DEF

Gold Nanoparticles

Monte Carlo method

Radiation dosimetry

Radiotherapy

### ABSTRACT

**Objective(s):** In this study we evaluate the impact of the different aspects of Gold Nano-Particles (GNPs) on the target absorptive Dose Enhancement Factor (DEF) during external targeted radiotherapy with photon beams ranging from kilovolt to megavolt energies using Monte Carlo simulation.

**Methods:** We have simulated the interaction of photon beams with various energies of radiation using water solution containing GNPs to be located in a tumor region and used MCNP5 code for Initially, the water phantom in which a tumor dimensions of  $1 \times 1 \times 1$  cm<sup>3</sup> was defined as the target, contained simulated GNPs. Then, the macroscopic DEF of GNPs of different sizes, including 15, 50, and 100 nm, had been calculated at the target area with a fixed concentration of 7 mg/g during external beam radiotherapy with single-energy photon beams ranging from keV to MeV.

**Results:** The tumor DEFs in the presence of GNPs were obtained 1.69-2.66 and 1.08-1.10 for keV and MeV beams, respectively. The highest DEF was achieved by photon energy of 50 keV. By increasing the size of the GNPs, the tumor dose factor raised too.

**Conclusions:** The factors calculated for enhancing the target dose of GNPs were in good agreements with previous studies based on keV photon energies. For MeV photon energies, after a reduction in the boundary between the two areas of water and the solution containing GNPs, the dose factor was enhanced to its maximum value for 2 and 6 MeV photon beams at the depths of 2.6 and 5.6 cm, respectively.

#### How to cite this article

Khosravi H, Mahdavi Gorabi A, Rahmani F, Ebadi A. The Impact of Nano-Sized Gold Particles on the Target Dose Enhancement Based on Photon Beams Using by Monte Carlo Method. *Nanomed Res J*, 2016; 1(2):84-89. DOI: 10.7508/nmrj.2016.02.004

### INTRODUCTION

With the development of nanotechnology, the radiosensitivity enhancement feature of nanoparticles such as GNPs has been applied to cancer cells. Nanoparticles exist in the form of colloidal solid particles in the sizes of 10 to 200 nm, which are 100 to 10,000 times smaller than human cells [1,2]. Nanoparticles smaller than 50nm can pass

\* Corresponding Author Email: [hkhosravi55@gmail.com](mailto:hkhosravi55@gmail.com)

easily through cell membranes. Nanoparticles have been used to treat cancer widely [3-9]. It seems that gold is the best choice for this purpose due to its adaptation to human body's biological environment [10-13]. In the interaction between X-ray and metal, nanoparticles create photo-electrons and secondary electrons. When these electrons interact with a biological tissue, they produce free radicals that can directly cause DNA strand breakage or

indirectly lead to a programmed cell death. In other words, GNPs can be considered as an extra source of free radicals. Therefore, it is expected that in the presence of GNPs, radiotherapy advantage enhances due to an increase in cell toxicity and destructive effect on cancer cells [14-16]. Ngwa *et al.* [17] studied the effect of radiation-sensitive properties of GNPs with dimensions of 50 nm on the cell (Hela) for brachytherapy sources using a low dose factor and energy. In this study, a source of <sup>125</sup>I was used for the cell (Hela) irradiation with and without GNPs. The results showed that the biological effects on Hela cells whereas irradiated in the presence of GNPs with a concentration of 2 mg/ml is about 70% to 130% higher compared to the absence of GNPs. Also, in lack of radiation, GNPs was represented at least effects on cancer cells.

In recent years, has been studied many times the use of GNPs in radiotherapy using empirical experiments and Monte Carlo simulation within cell cultures, animal models, and anthropoid phantoms [18-22]. In a study by Koger *et al.* [23], was evaluated the effects of GNPs on DEF in arc radiotherapy. In their research, the DEF was calculated using PENELOPE code and single-energy photons of 50-1000 keV and several energies used in the clinic. The DEFs of 40% and 25% were obtained for the energies of 100 keV and 6 MeV, respectively. Although the idea of increasing the dose by elements of high atomic numbers has been raised since a few decades ago, the adaptation of GNPs with biological systems has induced scientists to study more about the various applications of these materials in radiotherapy. The results of all the studies performed in this field have confirmed an increase in the dose reaching a tumor using radiotherapy with GNPs. However, the results of the interaction of radiation photon energies with the sizes of GNPs are still a controversial issue. For example in the Monte Carlo simulation and biological studies, GNPs with dimensions of about 10-100 nm and up to 1.9 nm have been utilized, respectively [1-9]. The most effective parameters on simulation using Monte Carlo method that have been reviewed and reported include dimensions larger than nanoparticles, high molar concentration, and low energy X- or gamma-ray photons that have provided more enhanced doses [18-23].

At energies higher than 1.02 MeV, a pair production phenomenon occurs that result in the production of pairs of electrons and positrons. Due to Compton scattering up to energy of 5 MeV, pair production under higher energies of 5 MeV would be the dominant process. In all the above interactions except for Compton scattering, cross-collision surfaces of photons depend on  $Z^4$  and  $Z^2.4$  in the photoelectric and pair production phenomena, respectively. Therefore, it is expected

that in the X- and gamma-ray interactions with gold atoms, considerable energies are transmitted to GNPs as free electrons and heat energy [24-25].

Dose Enhancement Factor (DEF) can be defined in terms of the ratio of mass absorption coefficient ( $\mu_{en}/\rho$ ) of gold to water. For single-energy beams, the DEF value is expressed as the following relation [26-27].

where NP is nanoparticles,  $\mu_{en}/\rho$  is the mass absorption coefficient of energy, WNP is the weight percentage of nanoparticles in the mixture, and E is the radiation beam single-energy. Controversial and sometimes different results can be seen in relation to the sensitive ability of gold nanoparticles in recent researches that could be resulted from performing studies under different conditions, including the particle geometry, size, and concentration, as well as the types of cell, radiation beam, and energy. In addition, in most previous studies conducted especially on GNPs with small dimensions, a mixture of gold atoms and water has been utilized instead of GNPs that cannot reflect the real conditions of the study issue [4-23].

We investigated MCNP5 code that use for simulation by Monte Carlo method. In this method applied statistical stochastic interactions for simulation of objects. In this study the actual impact of nano-sized gold particles created in tumor volume using iterative cells on the absorptive DEF in the target area/tumor during radiotherapy with single-energy photon beams within the varied range of energies from keV to MeV.

## MATERIALS AND METHODS

In this study, MCNP5 code was employed to simulate using Monte Carlo method. First, a water phantom with the dimensions of  $20 \times 20 \times 20$  cm<sup>3</sup> was simulated. In order to validate the simulation program, dosimetry parameters including percentage depth dose and transverse profiles calculated using a Monte Carlo code and then measurements obtained by a dosimeter of Farmer Ionization Chamber type (PTW Co.) with volumes of 15.0 mL and 6.0 mL for areas before and after aggregation that were compared, respectively. To this goal, the quantities of percentage depth dose and transverse profiles of Varian linear accelerator device for a square field with the dimensions of  $10 \times 10$  cm<sup>2</sup> (the reference field size in conventional radiotherapies) were measured with energies of 6 and 18 MeV by the mentioned dosimeter and compared with the values calculated by a Monte Carlo code. Furthermore, the parameter of dose difference in percentage was used for the comparison of the percentage depth dose with the low-dose gradients of transverse profiles and also the parameter of distance-to-agreement in millimeters with the high-dose gradients of

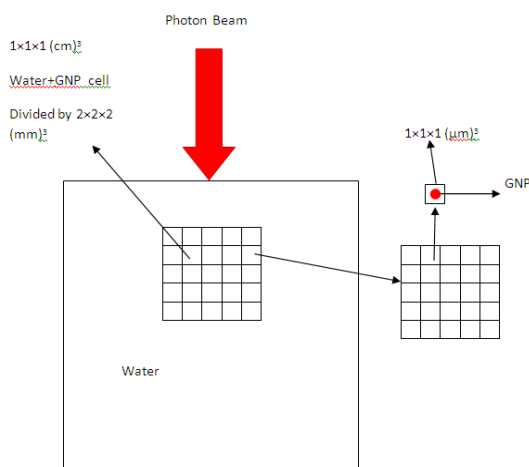


Fig. 1. A schematic view of the geometry simulated via MCNP5 code

the profiles was utilized to compare the dose distribution calculated by the corresponding values measured. For comparing the simulation program with actual measurements, the quantity of local dose difference percentage was employed according to the following relation: Local dose difference =  $100 \times (|DoseCalculation - Dose Measurement| / DoseMeasurement)$ .

The difference percentage between the measured values of percentage depth dose from those calculated at the depths of deeper than the aggregation area was less than 1%. This difference at the depths of less than the aggregation area increased to 3%. The maximum distance-to-agreement was 1.5 mm for an energy of 18 MeV. Given the above values, the differences obtained were within the recommended limit of acceptable error [28- 29].

A cube-shaped tumor with three dimensions of  $1 \times 1 \times 1$  cm at a depth of 5 cm and a water phantom surface were simulated for MeV and keV beams, respectively. To perform the simulation, spherical GNPs were uniformly distributed within the tumor mass. To do this, using iterative structures, the tumor mass was divided into networks of dimensions  $2 \times 2 \times 2$  mm<sup>3</sup>. Cards LAT = 1 and LAT = 2 could be used for cubic and octagonal prismatic networks, respectively. The mentioned cards are employed together with FILL and U cards when defining the cell. A world can be a regular or normal network of cells. The non-zero value entered for card U is similar to that given to card FILL of the cell to which the world belongs. Card FILL indicates that the desired cell has been filled by the cells possessing card U. The cells of a world can be finite or infinite, but they must fill all the space inside the cell. Lack of using card U or a value of zero for it means that the cell does not belong

to any worlds. The values of the world are integers and to be selected by the user as desired [30]. Then, each of these 2-mm networks were divided into smaller networks with the dimensions of  $1 \times 1 \times 1$  μm<sup>3</sup>. Subsequently, GNPs with the dimensions of 15, 50, and 100 nm were placed at the centers of 1-micron networks. The distribution method of these nanoparticles is shown in Fig. 1.

It should be noted that for smaller nanoparticles (15 and 50 nm), the internal networks were divided into dimensions smaller than 1 μm<sup>3</sup> so as to obtain the desired concentration of 7 mg/g.

In these simulations, for keV and MeV modes, mono-energetic photon beams of 0.05, 0.09, 2, and 6 MeV were used, respectively. The distance from the source to the surface was considered to be 25 and 100 cm for keV and MeV modes, respectively. In the simulation carried out using MCNP5 code, each photon history was pursued up to an energy of 1 keV. A statistical error of less than 1% was achieved for 108 particle histories in all the simulations.

## RESULTS

The absorptive DEFs of GNPs with different dimensions at 50 and 90 keV energies are shown in (Figs. 2). As can be seen in these Figs, the absorptive DEFs raise by increasing the diameters of GNPs. In (Figs. 3), the absorptive DEFs of GNPs of 50 nm are displayed in 2 and 6 MeV energies. The exceeding depth can cause increasing and decreasing of DEFs (Figs. 3).

The DEF averages of GNPs with different energies and dimensions are exhibited in Table 1. As can be seen in this table, DEF amount rises by increasing the diameters of GNPs in a keV mode. The highest (DEF 2.66) was obtained for GNPs with a dimension of 100 nm at 50 keV. In a MeV mode, no significant changes were observed in the value of DEF by increasing the diameters of GNPs. However, by increasing energy, DEF levels were enhanced so that the highest DEF of 1.10 was obtained at 6 MeV.

At low energies (50 and 90 keV), the photoelectric phenomenon is the dominant effect for the absorptive DEF in the presence of GNPs. At higher energies (2 and 6 MeV), the Compton and pair production phenomena have a direct impact on the absorptive DEF.

## CONCLUSION

In most previous studies, a mixture of gold atoms with water has been used instead of GNPs, which cannot express the real conditions of the study issue [4-23]. Yet, in this study, despite low concentrations of GNPs (0.7 weight percentage) a higher relative DEF was obtained compared to similar studies [20], which was due to GNPs as

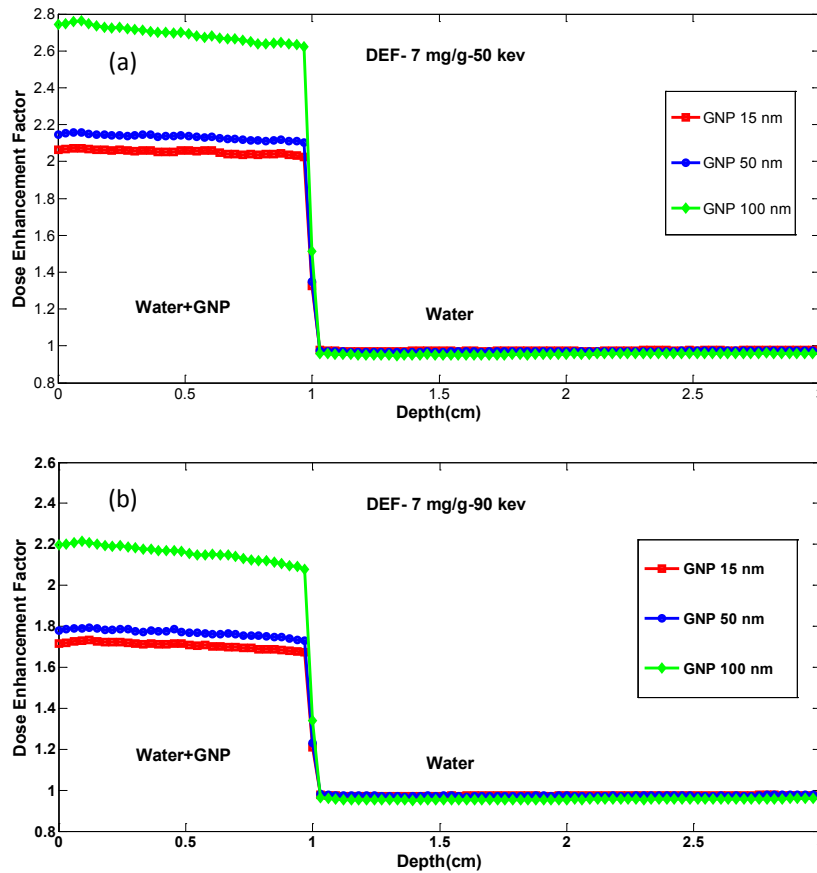


Fig. 2. The absorptive DEFs for GNPs with different dimensions: (a) energy of 50 keV, (b) energy of 90 keV

a real situation ( i.e. the use of micron networks in which GNPs were placed). In other words, by this method, there is a higher probability of interactions between radiation photons and gold atoms changed as a condensed matter compared to a state in which gold atoms are distributed uniformly in the water. Therefore, the amount of energy transferred to the environment in this case is greater than the state in which gold atoms are uniformly distributed. Moreover, less work has been done at high energies in this area, while their effects on the absorptive EDF levels were studied in this paper. The phenomenon of pair production is the effective parameter on the absorptive EDFs within the mentioned range (MeV).

Table 1. Average DEFs for different energies in the presence of GNPs with different sizes

Beam energy	GNP Dimensions (nm)		
	15	50	100
50 keV	2.03	2.11	2.66
90 keV	1.69	1.75	2.13
2 MeV	1.07	1.08	1.08
6 MeV	1.09	1.09	1.10

At high energies, nearly all the electrons created by Compton phenomenon move along the radiation photons and release their energies at a distance farther than the tumor surface. On the contrary, on the border between the two environments where the absorptive dose should be increased [31], an initial dose reduction is witnessed within the interval of the two environments of water and aqueous solution containing GNPs (Figs 3). This phenomenon may be due to the natures of GNPs and behaviors of colliding. In other words, since GNPs are denser than typical huge gold, the high-energy photons colliding with it produce high-energy electrons that gradually release their energies in relatively remote depths from their places of production as moving through the matter. Because of the large number of GNPs in the tumor, the electron flux and thus the absorbed dose enhances with increasing depth until it reaches its maximum value. Furthermore, by reducing the intensity of the photon beams, productions of secondary electrons decrease resulting in a gradual dose reduction at more depths.

In the pair production phenomenon, the electrons and positrons created release their energies

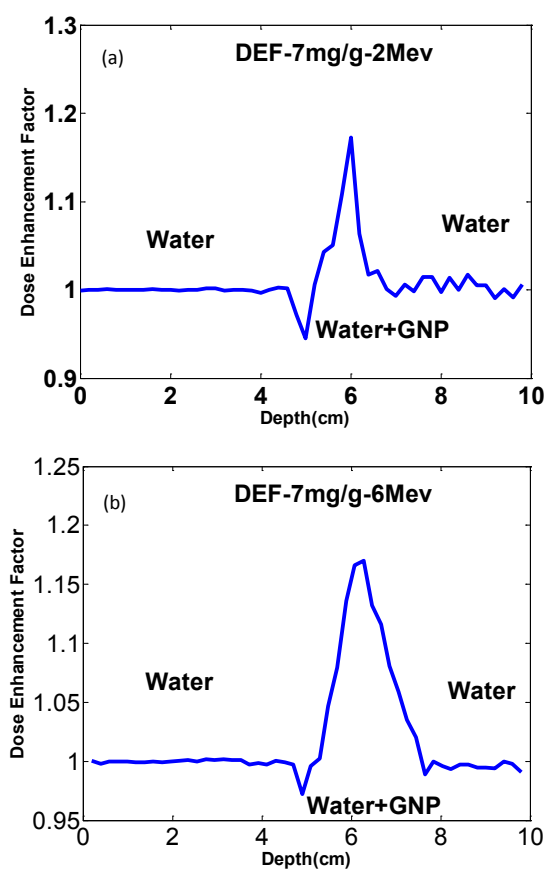


Fig. 3. The absorptive DEFs for GNPs of 50 nm: (a) energy of 2 MeV, (b) energy of 6 MeV

at a shorter distance than their places of production when colliding with GNPs. This phenomenon is further manifested at higher energies like 6 MeV (Fig. 3(b)). At the maximum half, the width at an energy of 6 MeV is more than that of 2 MeV (Figs. 3). The reason for this phenomenon would be the higher rate of pair production at the energy 6 MeV compared to that of 2 MeV.

In recent years, the use of GNPs in radiotherapy has been many times studied by various empirical experiments and Monte Carlo simulation. Although the idea of dose enhancement by elements with high atomic numbers has been raised since several decades ago, the adaptation of GNPs with biological systems has encouraged scientists to investigate more about the various applications of these materials in radiotherapy. The results of all the studies in this field have confirmed an enhanced dose reaching the tumor through radiotherapy with GNPs. Nevertheless, the results of the interactions of radiation energies with different sizes of GNPs are still controversial. In other words, the results of empirical experiments and Monte Carlo simulations for GNPs of similar

dimensions have been different [18-23]. Thus, to achieve a unified theory and consensus in this field, more experiments and calculations should be performed on different cells and animal models. In this study, we have tried to somewhat answer the questions raised. Yet, our results have been limited to a range of energies and particle sizes as well as simulation conditions under study. Obviously, to achieve a global consensus on clinical application, further and wider research is essential in this regard.

#### CONFLICTS OF INTEREST

The authors declare that there are no conflicts of interest regarding the publication of this manuscript.

#### REFERENCE

- Hainfeld JF, Slatkin DN, Smilowitz HM. The use of gold nanoparticles to enhance radiotherapy in mice. *Phys Med Biol.* 2004;49(18):N309.
- Yih TC, Wei C. Nanomedicine in cancer treatment. *Nanomed Nanotech Biol Med.* 2005;1(2):191-2.
- Kawasaki ES, Player A. Nanotechnology, nanomedicine, and the development of new, effective therapies for cancer. *Nanomed Nanotech Biol Med.* 2005;1(2):101-9.
- Van den Heuvel F, Locquet J-P, Nuyts S. Beam energy considerations for gold nano-particle enhanced radiation treatment. *Phys Med Biol.* 2010;55(16):4509.
- Butterworth KT, Coulter J, Jain S, Forker J, McMahon S, Schettino G, et al. Evaluation of cytotoxicity and radiation enhancement using 1.9 nm gold particles: potential application for cancer therapy. *Nanotechnology.* 2010;21(29):295101.
- Toossi MTB, Ghorbani M, Mehrpouyan M, Akbari F, Sabet LS, Meigooni AS. A Monte Carlo study on tissue dose enhancement in brachytherapy: a comparison between gadolinium and gold nanoparticles. *Australas Phys Eng Sci Med.* 2012;35(2):177-85.
- Coulter JA, Jain S, Butterworth KT, Taggart LE, Dickson GR, McMahon SJ, et al. Cell type-dependent uptake, localization, and cytotoxicity of 1.9 nm gold nanoparticles. *Int J Nanomedicine.* 2012;7(1).
- Jain S, Hirst D, O'sullivan J. Gold nanoparticles as novel agents for cancer therapy. *Br J Radiol.* 2012;85(1010):101-13
- Cruje C, Chithrani B. Integration of peptides for enhanced uptake of PEGylated gold nanoparticles. *J Nanosci Nanotechnol.* 2015;15(3):2125-31.
- Hirsch LR, Stafford R, Bankson J, Sershen S, Rivera B, Price R, et al. Nanoshell-mediated near-infrared thermal therapy of tumors under magnetic resonance guidance. *Proc Natl Acad Sci.* 2003;100(23):13549-54.
- Berbeco RI, Korideck H, Kumar R, Sridhar S, Detappe A, Ngwa W, et al. Targeted Gold Nanoparticles as Vascular Disrupting Agents During Radiation Therapy. *Int J Radiat Oncol Biol Phys.* 2014;90(1):S198.
- Wolfe T, Chatterjee D, Lee J, Grant JD, Bhattarai S, Taylor R, et al. Targeted gold nanoparticles enhance sensitization of prostate tumors to megavoltage radiation therapy in vivo. *Nanomed Nanotech Biol Med.* 2015;11(5):1277-83.
- Rengan AK, Bukhari AB, Pradhan A, Malhotra R, Banerjee R, Srivastava R, et al. In vivo analysis of biodegradable liposome

- gold nanoparticles as efficient agents for photothermal therapy of cancer. *Nano Lett.* 2015;15(2):842-8.
14. Loo C, Lowery A, Halas N, West J, Drezek R. Immunotargeted nanoshells for integrated cancer imaging and therapy. *Nano Lett.* 2005;5(4):709-11.
  15. Jain S, Coulter JA, Hounsell AR, Butterworth KT, McMahon SJ, Hyland WB, et al. Cell-specific radiosensitization by gold nanoparticles at megavoltage radiation energies. *Int J Radiat Oncol Biol Phys.* 2011;79(2):531-9.
  16. Zhang X-D, Wu D, Shen X, Chen J, Sun Y-M, Liu P-X, et al. Size-dependent radiosensitization of PEG-coated gold nanoparticles for cancer radiation therapy. *Biomaterials.* 2012;33(27):6408-19.
  17. Ngwa W, Korideck H, Kassis AI, Kumar R, Sridhar S, Makrigiorgos GM, et al. In vitro radiosensitization by gold nanoparticles during continuous low-dose-rate gamma irradiation with I-125 brachytherapy seeds. *Nanomed Nanotech Biol Med.* 2013;9(1):25-7.
  18. Cho SH. Estimation of tumour dose enhancement due to gold nanoparticles during typical radiation treatments: a preliminary Monte Carlo study. *Phys Med Biol.* 2005;50(15):N163-73.
  19. Zhang SX, Gao J, Buchholz TA, Wang Z, Salehpour MR, Drezek RA, et al. Quantifying tumor-selective radiation dose enhancements using gold nanoparticles: a monte carlo simulation study. *Biomed Microdevices.* 2009;11(4):925-33.
  20. Cho SH, Jones BL, Krishnan S. The dosimetric feasibility of gold nanoparticle-aided radiation therapy (GNRT) via brachytherapy using low-energy gamma/x-ray sources. *Phys Med Biol.* 2009;54(16):4889.
  21. Leung MKK, Chow JCL, Chithrani BD, Lee MJG, Oms B, Jaffray DA. Irradiation of gold nanoparticles by x-rays: Monte Carlo simulation of dose enhancements and the spatial properties of the secondary electrons production. *Med Phys.* 2011;38(2):624-31.
  22. Lechtman E, Mashouf S, Chattopadhyay N, Keller BM, Lai P, Cai Z, et al. A Monte Carlo-based model of gold nanoparticle radiosensitization accounting for increased radiobiological effectiveness. *Phys Med Biol.* 2013;58(10):3075.
  23. Koger B, Kirkby C. Sci—Thur AM: YIS-04: Gold Nanoparticle Enhanced Arc Radiotherapy: A Monte Carlo Feasibility Study. *Med Phys.* 2014;41(8):1-2.
  24. Khan FM, Gibbons JP. Khan's the physics of radiation therapy: Lippincott Williams & Wilkins; 2014.
  25. Gasiorowicz S. Quantum physics. Hoboken, NJ: John Wiley & Sons; 2007.
  26. Esteve F, Corde S, Elleaume H, Adam JF, Joubert A, Charvet AM, et al. Enhanced radio sensitivity with iodinated contrast agents using monochromatic synchrotron X-rays on human cancerous cells. *Acad Radiol.* 2002;9(2):S540-S3.
  27. Corde S, Joubert A, Adam JF, Charvet AM, Le Bas JF, Esteve F, et al. Synchrotron radiation-based experimental determination of the optimal energy for cell radiotoxicity enhancement following photoelectric effect on stable iodinated compounds. *Br J Cancer.* 2004;91(3):544-51.
  28. Almond PR, Biggs PJ, Coursey BM, Hanson WF, Huq MS, Nath R, et al. AAPM American Association of Physicists in Medicine, Task Group 51: Protocol for clinical reference dosimetry of high-energy photon and electron beams. *Med Phys.* 1999;26:1847-70.
  29. AGENCY IAE. Implementation of the International Code of Practice on Dosimetry in Radiotherapy (TRS 398): Review of Testing Results. Vienna: INTERNATIONAL ATOMIC ENERGY AGENCY; 2010.
  30. Kiedrowski B, Brown F, Bull J. MCNP5-1.6, Feature Enhancements and Manual Clarifications. LA-UR-10-06217. 2010.
  31. Greening JR. Fundamentals of radiation dosimetry: CRC Press; 1985.